Morphine regulates expression of MOR-1A, an intron-retention carboxyl terminal splice variant of the mu opioid receptor (*OPRM1*) gene via miR-103/miR-107

Zhigang Lu, Jin Xu, Mingming Xu, Gavril W Pasternak, Ying-Xian Pan

Department of Neurology and the Molecular Pharmacology and Chemistry Program,

Memorial Sloan-Kettering Cancer Center, New York, NY 10065, USA

Running title: Morphine regulates MOR-1A expression via miR-103/107

Address correspondence to:

Dr. Ying-Xian Pan, Department of Neurology, Memorial Sloan-Kettering Cancer Center,

1275 York Avenue, New York, NY 10065. E-mail: pany@mskcc.org. Telephone: 646-

888-2167; Fax: 646-422-0271

Text pages: 39

Tables: None

Figures: 8

References: 67

Words in the Abstract: 236

Words in the Introduction: 730

Words in the Discussion: 1176

Abbreviations:

OPRM1, mu opioid receptor; MOR-1, mu opioid receptor; 3'-UTR, 3'-untranslated

region; poly(A), polyadenylation; RACE, rapid amplification cDNA ends;

Abstract

The μ opioid receptor (MOR-1) gene, *OPRM1*, undergoes extensive alternative splicing, generating an array of splice variants. Of these variants, MOR-1A, an intron-retention carboxyl terminal splice variant identical to MOR-1 except for the terminal intracellular tail encoded by exon 3b, is quite abundant and conserved from rodent to humans. Increasing evidence indicates that miroRNAs (miRNAs) regulate MOR-1 expression and μ agonists such as morphine modulate miRNA expression. However, little is known about miRNA regulation of the *OPRM1* splice variants. Using 3' rapid amplification cDNA end (RACE) and Northern blot analyses, the present study identified the complete 3' untranslated region (3'-UTR) for both mouse and human MOR-1A and their conserved polyadenylation site, and defined the role the 3'-UTR in mRNA stability using a luciferase reporter assay. Computer models predicted a conserved miR-103/107 targeting site in the 3'-UTR of both mouse and human MOR-1A. The functional relevance of miR-103/107 in regulating expression of MOR-1A protein through the consensus miR-103/107 binding sites in the 3'-UTR was established by using mutagenesis and a miR-107 inhibitor in transfected HEK293 cells and Be(2)C cells that endogenously express human MOR-1A. Chronic morphine treatment significantly upregulated miR-103 and miR-107 levels, leading to downregulation of polyribosome-associated MOR-1A in both Be(2)C cells and the striatum of a morphine tolerant mouse, providing a new perspective on understanding the roles of miRNAs and *OPRM1* splice variants in modulating the complex actions of morphine in animals and humans.

Introduction

Morphine and most clinical analgesic agents act through mu opioid receptors. Pharmacological studies have defined several mu receptor subtypes including mu_1, mu_2 and morphine-6β-glucuronide (M6G) receptors(Wolozin and Pasternak, 1981;Reisine and Pasternak, 1996;Pasternak, 1993;Rossi et al., 1996;Rossi et al., 1995). However, a single mu opioid receptor gene (*OPRM1*) has been identified in all the species (Min et al., 1994;Giros et al., 1995;Liang et al., 1995), raising the possibility of alternative pre-mRNA splicing of the *OPRM1* gene to generate multiple splice variants with diverse actions. This concept is supported by antisense mapping studies(Rossi et al., 1995;Rossi et al., 1997), the isolation of an array of splice variants in mouse, rat and human(Pan, 2005;Pasternak and Pan Y-X., 2013), and gene targeting studies(Schuller et al., 1999;Pan et al., 2009;Majumdar et al., 2011b).

The *OPRM1* splice variants can be categorized into three groups based upon their structure, full length carboxyl (C-) terminal variants with 7 transmembrane (TM) domains, truncated 6-TM variants and single TM variants. All the full length C-terminal splice variants have identical transmembrane domains, which are encoded by exons 1, 2 and 3 and comprise the binding pocket, but contain a different intracellular C-terminal tail encoded by alternative 3' exons. Growing evidence suggests the functional importance of these C-terminal splice variants based upon region-specific expression(Abbadie et al., 2000b;Abbadie et al., 2000a;Abbadie et al., 2001;Pan et al., 1999;Pan et al., 2001), agonist-induced G protein coupling(Bolan et al., 2004;Pasternak et al., 2004;Pan et al., 2005a;Pan et al., 2005b), receptor phosphorylation(Koch et al.,

2001), internalization(Koch et al., 1998;Koch et al., 2001), post-endocytic

sorting(Tanowitz et al., 2008), and morphine-induced itch(Liu et al., 2011).

The first reported C-terminal splice variant was the human MOR-1A (hMOR-

1A)(Bare et al., 1994), followed soon afterwards by the mouse and rat homologues,

mMOR-1A and rMOR-1A (Bolan et al., 2004;Pasternak et al., 2004) (Fig. 1). All these

MOR-1A's are intron retention variants in which the 5' splice donor site at the end of

exon 3 is skipped, leading to retention of exon 3b, that is a part of an intron in the other

splice variants. Continuous translation from exon 3a to exon 3b predicts four amino

acids, VRSL in hMOR-1A and mMOR-1A and VCAF in rMOR-1A, before encountering a

same TAG stop codon(Pasternak et al., 2004;Xu et al., 2013). Similar to other *OPRM1*

splice variants, mMOR-1A mRNA is differentially expressed in various brain regions (Xu

et al., 2013). When expressed in Chinese Ovary Hamster (CHO) cells, mMOR-1A and

rMOR-1A display high mu binding affinity and selectivity(Bolan et al., 2004;Pasternak et

al., 2004;Xu et al., 2013). However, they revealed marked differences in agonist-

induced total G protein stimulation determined by $[^{35}S]\gamma GTP$ binding as compared with

other C-terminal splice variants(Bolan et al., 2004;Pasternak et al., 2004;Xu et al.,

2013), suggesting the functional significance of the C-terminal tails in agonist-induced G

protein coupling and signaling transduction.

Pre-mRNA 3'-end processing in most eukaryotic genes involves cleavage and

polyadenylation through conserved cis-elements in the 3' untranslated region (3'-UTR),

and is tightly coupled to transcription, splicing, transport from the nucleus to the

cytoplasm and translation, as well as influencing mRNA stability (Mandel et al.,

2008;Elkon et al., 2013;Tian and Manley, 2013). The complete 3'-UTR containing

poly(A) signal and cleavage site of the original human and mouse MOR-1 was identified(Ide et al., 2005;Wu et al., 2005). However, little is known for the 3'-UTR of the *OPRM1* splice variants including MOR-1A.

MicroRNAs (miRNAs) are a class of small non-coding RNAs that bind to target mRNAs to regulate their stability and translation. Mu opioids such as morphine modulated expression of a number of miRNAs(Sanchez-Simon et al., 2010;Zheng et al., 2010;Wu et al., 2009;Wu et al., 2008;Dave and Khalili, 2010;Wang et al., 2011;Wu et al., 2012;He et al., 2010), and several miRNAs regulated MOR-1 expression(Wu et al., 2009;Wu et al., 2008;Wu et al., 2012;He et al., 2010). Dysregulation of miRNAs has been linked to morphine tolerance and addiction(He et al., 2010;Hwang et al., 2011;Dreyer, 2010;Tapocik et al., 2012). Yet, there has been a lack of information regarding miRNA regulation of the *OPRM1* splice variants. In the present study, we isolated the complete 3'-UTRs of hMOR-1A and mMOR-1A that contain the cleavage and poly(A) signal sites and identified a pair of paralogous miRNAs, miR-103 and miR-107, that regulate expression of hMOR-1A and mMOR-1A post-transcriptionally through a conserved miR-103/107 binding site in the 3'-UTRs. We further demonstrated that morphine altered the expression of hMOR-1A in Be(2)C cells and mMOR-1A in the striatum of morphine tolerance mice via miR-103 and miR-107.

Materials and Methods

3'-Rapid amplification cDNA ends (RACE) and sequencing. Total RNAs were extracted from HEK293, Be(2)C cells and mouse brain with TRI Reagent (Life Technologies, Norwalk, CT). Poly(A) plus RNA was then isolated from the total RNAs

using MicroPoly(A) Purist (Ambion, Austin, TX), and used in 3'-RACE mainly following

the protocol described in the 3'-RACE Kit (Clontech, Mountain View, CA) with some

modification. Briefly, the first-strand cDNA was synthesized by using mRNA as

template, 3'RACE primer (5'-CCA TCC TAA TAC GAC TCA CTA TAG GGC TCG AGC

GGC TTT TTT TTT TTT TTT TTT TTT TTT TTT TTT VN-3') and SuperScript III (Life

Technologies), and used in the first-round PCR with a sense primer for mouse, mA (5-

CAG ACT GTT TCCTGG CAC TTC TGC ATT GCC TTG GGT TAC AC-3) or for

human, hA (5'-CAT CCA ACC TGG TAC TGG GAA AAC CTG-3') and an antisense

primer, AP1 (5'-TAG CTT AAC TCG GAA CTG AGT-3'). The first-round PCR product

was then used in the second-round or nested PCR with a sense primer for mouse, mB

(5'- CTC CGC AGG TTC TAG CAG TGG GCG TGG CAG AAC GAA TG-3') or for

human, hB (5'-GGA AGC AAA TTG TGG TTC TAG TGT TAG AGA AG-3') and an

antisense primer, AP2 (5'-ACT CAC TAT AGG GCT CGA GCG GC-3'). PCRs were

performed with Platinum Taq DNA polymerase under conditions consisting of a 2min

denaturing at 95°C and 39 cycles of amplification at 95°C for 20 sec, 65°C for 30 sec,

and 72°C for 1 min followed by 8 min extension at 72°C. PCR products from the 2nd

PCRs were separated in a 1.5% agarose gel. Amplified cDNA fragments were extracted

by gel extraction kit (QIAGEN, Valencia, CA), and sequenced with the primers used in

PCR in both orientations.

Northern blot analysis. Northern blot analysis was performed as described

previously(Pan et al., 2001) with minor modifications. Briefly, 3 μg of poly(A) plus RNA

was separated on a 0.8% formaldehyde agarose gel and transferred to a GenePlus

7

membrane. After pre-hybridized in Ultra hybridization buffer (Ambion) at 42°C for 2 hr, membrane was then hybridized with ^{32}P-labeled cDNA probes in Ultra hybridization buffer at 42°C overnight, washed sequentially with High-stringent and Low-stringent washing buffers (Ambion), and exposed to Kodak BioMax MS film. Images were captured using ChemiDoc MP system (Bio-Rad, Hercules, CA). ^{32}P-labeled probes were generated by PCRs with following primers: mouse probe 1 (415 bp) located at exon 3a, sense primer (5'-TGC TCA AAA TCT GTG TCT TCA TCT TCG CCT TCA TC-3') and antisense primer (5'-GTT TTG ACG GAT TCG AGC AGA GTT TTG C-3'); mouse probe 2 (143 bp) located at exon 3b, sense primer (5'-GGA GTC T GA AC ACT AGA GCA AAT GCC AGC-3') and antisense primer (5'-CTT GGG ACT CTC CTG GGC ATA GTA ATA CAT G-3'); mouse probe 3 (439 bp) located at downstream of the cleavage site, sense primer (5'-CAA AAT CCT TCC CAC ACC TAA AAA TCA CTG-3') and antisense primer (5'-GAA TGA ATC TGC CAC CAT TAC CAC CAT G-3'); human probe 1 (427 bp) located at exon 3a, sense primer (5'-CAT CCA ACC TGG TAC TGG GAA AAC CTG-3') and antisense primer (5'- CGA GTG GAG TTT TGT TGC TCA ATG TTG G-3'); human probe 2 (291 bp) located at exon 3b, sense primer (5'-GGA AGC AAA TTG TGG TTC TAG TGT TAG AGA AG-3') and antisense primer (5'-CCA GAG CAA GAC TGG CTT TTG AGA AAT AAG-3'); human probe 3 (331 bp) located at downstream of the cleavage site.

Plasmid Constructs. To generate pmir without poly(A) construct (pNo-3'UTR), the SV40 poly(A) sequence was deleted from pmirGLO Vector (Promega, Madison, WI) by using Chang-IT^{TM} Mutagenesis kit (Affymetrix, Santa Clara, CA) with a mutagenesis

8

primer (5'-CAT AAC CCC TTG GGG CGG CCG CTT CGA GCG GCC GGC CTA TCC CGG GAA ATC GAA TTT TAA CAA AAT ATT AAC GC-3'). A 752 bp of hMOR-1A 3'-UTR (human PCR fragment) and a 1,761 bp of mMOR-1A 3'-UTR fragments (mouse PCR fragment) were amplified by PCRs with a sense primer and an antisense primer flanking with NheI and XhoI sites, respectively. The primers for amplifying hMOR-1A 3'-UTR were: a sense primer, 5'-GGC GCT AGC GGT ACG CAG TCT CTA GAA TTA GGT ATA TCT ACT GGG-3' and an antisense primer, 5'-CCG CTC GAG GTG TGT ATA AGT CTT GAA TTT TCT GTG TAG GTC TGG-3'; and for amplifying mMOR-1A 3'-UTR, a sense primer, 5'-GGC GCT AGC GTA TGT GCT TTC TAG AAT TAT GTA TAA CAT ATA AAA ACA CAG-3', and an antisense primer, 5'-CCG CTC GAG GGG AAT GAA TCT GCC ACC ATT ACC ACC-3'. The digested PCR fragments with NheI and XhoI were subcloned into pNo-3'UTR to generate pmir with hMOR-1A 3'-UTR (pH-3'UTR) and mMOR-1A 3'-UTR (pM-3'UTR) constructs. To generate pmir constructs with hMOR-1A (pH-wt) or mMOR-1A 3'-UTR (pM-wt) containing wide-type (wt) miR-103/107 sequence, the human and mouse PCR fragments (see above) were subcloned into NheI and XhoI sites of pmirGlo Vector containing the original SV40 poly(A). The wt miR-103/107 sequences in pH-wt and pM-wt constructs were disrupted by mutagenesis using Chang-IT^{TM} Mutagenesis kit with a mutagenesis primer for mouse (M103/107-mut) , 5'-GGG GAG GGG AGA CTA TAG ACA GAA GUC CAC CGG AAG ATU GAA AGT TAC TAT CCT CAG-3', or for human (H103/107-mut), 5'-CAT TTT CCC CAG AAT TAT TAT ATG ACT AGC GTG CTG CAG TAG GTA CCC CTC TTA TTT CTC-3', to generate pM-mut and pH-mut, respectively. The mutagenesis strategy was to not only change seed sequences, but also mutate other non-seed sequences. To generate

9

pcDNA3 constructs containing hMOR-1A and mMOR-1A coding region and their 3'-UTRs (ph1A/wt and hm1A/wt), the hMOR-1A and mMOR-1A 3'-UTRs were amplified with the following primers flanking with XhoI and XbaI sites (human sense primer, 5'-CCG CTC GAG GGT ACG CAG TCT CTA GAA TTA GGT ATA TCT ACT GGG-3'; human antisense primer, 5'- CCG TCT AGA GTG TGT ATA AGT CTT GAA TTT TCT GTG TAG GTC TGG-3'; mouse sense primer, 5'- CCG CTC GAG GTA TGT GCT TTC TAG AAT TAT GTA TAA CAT ATA AAA ACA CAG-3'; mouse antisense primer, 5'- CCG TCT AGA GTG TAT GTG CTT TCT AGA ATT ATG TAT AAC ATA TAA AAA CAC AG-3'), and subcloned into the original hMOR-1A and mMOR-1A cDNA constructs (Pan et al., 2005a;Bolan et al., 2004) in pcDNA3 with XhoI and XbaI, respectively. The same mutagenesis primers, H103/107-mut and M103/107-mut used above, were used in mutagenesis using ph1A/wt and pm1A/wt as templates to make ph1A/mut and pm1A/mut that were identical to ph1A/wt and pm1A/wt except that the miR-103/107 sequences were disrupted.

Cell Culture, transfection, morphine treatment and Luciferase Reporter Assay.

Human embryonic kidney (HEK293) and Be(2)C cells were maintained in DMEM supplemented with 10% fetal bovine serum (FBS) and non-essential amino acids (NEAA), and MEM supplemented with 10% FBS and NEAA, respectively, in an atmosphere of 5% CO_2 at 37°C. Plasmid constructs were transfected into HEK293 cells plated in 48-well or 6-well plates using the Effectene reagent (QIAGEN, German) following the manufacture's protocol. Antisense locked nucleic acid (LNA) oligonucleotide against miR107 (miR-107 inhibitor, 5'-GAT AGC CCT GTA CAA TG-3',

Exiqon, Denmark) with or without plasmid constructs was transfected with lipofactamine

2000 (Life Technologies) into HEK293 cells following the manufacture's protocol. A

negative control LNA oligonucleotide (5'-GTG TAA CAC GTC TAT ACG CCC A-3',

Exiqon) was used as a control. NeuroMag reagent (OZ Bioscience, France) was used to

transfect miR-107 inhibitor into Be(2)C cells following the manufacture's protocol.

Be(2)C cells were treated with morphine at the indicated concentrations for 48 hr in the

presence or absence of control LNA oligo (5nM) or miR-107 inhibitor (5nM). After 48h of

transfection, cells were washed with phosphate-buffered saline(PBS) and lysed with

lysis buffer provided from Dual-Glo Luciferase Assay Kit (Promega). Cleared lysate was

used to determine the luciferase activities by using the Dual-Glo Luciferase Assay

Reagents in TD-20/20 luminometer (Promega). Luciferase activity was calculated by

normalizing with Renilla luciferase activity obtained from the same assay.

Animal and chronic morphine treatment. C56BL/6J (B6, stock #: 000664) male mice

at 7 - 8 weeks of age were obtained from Jackson Laboratory. All mice were housed in

groups of five, maintained on a 12-h light/dark cycle and given ad libitum access to food

and water. All animal studies were approved by the Institutional Animal Care and Use

Committee of the Memorial Sloan-Kettering Cancer Center. Chronic morphine treatment

with morphine pellet (75 mg of free base) and placebo pellet (a gift from the Research

Technology Branch of the National Institute on Drug Abuse (Rockville, MD)) was

performed as previously described (Kolesnikov et al., 1993). Briefly, pellets were

subcutaneously (s.c.) implanted into the back of mice under oxygen/isoflurane inhalant

anesthesia. All mice implanted with morphine pellet showed morphine tolerance after

11

the 3-day implantation, while mice with placebo pellet displayed normal morphine

analgesia (data not shown), as determined by the radiant heat tail-flick assay. On the

fourth day, mice were sacrificed, and the prefrontal cortex and striatum were dissected

for isolating total RNA and polysome-associated mRNA (see below).

Isolation of polyribosome (polysome) and RNA extraction. Polysomal fraction was

obtained following the previously described procedures (Wu and Bag, 1998) with minor

modification(Thoreen et al., 2012). Briefly, HEK cells or Be(2)C cells in 6-well plates

were then treated with 100µg/ml cycloheximide at 37°C for 10 min, washed in ice-cold

PBS containing 100µg/ml cycloheximide, and lysed in Polysome Lysis buffer (15mM

HEPES-KOH, pH 7.4, 7.5mM $MgCl_2$, 100mM KCl, 2mM DTT, and 1.0% Triton X-100)

containing 100µg/ml cycloheximide and EDTA-free protease inhibitors (Roche) by

homogenizing with a 26-gauge needle for six times at 4 °C. 1/10 volume of lysate was

used for total RNA extraction by using miRNeasy Kit (Qiagen). The rest lysate was

centrifuged at 1,0000g for 10 min, and the supernatant was then centrifuged in an SW-

41Ti rotor at 100,000 x g. for 1 h. The pellet as polysome fraction was used for RNA

extraction by using miRNeasy Kit. Isolation of polysome fraction from the dissected

mouse PFC and striatum was identical to those from the cell lines except that dissected

regions were immediately homogenized with a Dounce homogenizer in Polysome Lysis

buffer containing 100µg/ml cycloheximide and EDTA-free protease inhibitors. RNA

concentration was determined by using Qubit RNA assay in a Qubit 2.0 Fluoreometer

(Life Technologies).

Reverse-transcription-quantitative polymerase chain reaction (RT-qPCR).

Total RNA and polysomal mRNA were reverse-transcribed by using Superscript III and

random hexamer. The first-stand cDNA was then used as template in SYBR green

qPCR with HotStart-IT SYBR Green qPCR Master Mix (Affymetrix) in a MJ Opticon 2

qPCR machine. The following primers were used: for luc2 mRNA, sense primer, (5'-

GAT AGC AAG ACC GAC TAC CAG GGC TTC-3') and antisense primer, (5'-CGG ACA

CAA GCG GTG CGG TG-3'); for mMOR-1A, sense primer, (5'-CAC AAA ATA CAG

GCA GGG GTC CA-3') and antisense primer, (5'-CTA AAT CTT AGA CTG GTA TCA

GGT GCT GTG-3'); for hMOR-1A, sense primer, sense primer, (5'-CAA AAT ACA GGC

AAG GTT CCA TAG ATT G -3') and antisense primer, (5'-CAT CCC CAG TAG ATA

TAC CTA ATT CTA GAG AC-3'). The qPCRs were performed by initial 2 min at 95°C,

followed by 45 cycles of 95°C for 15 sec, 65°C for 15 sec, and 72°C for 30 sec (luc2

mRNA) or 60 sec (mMOR-1A or hMOR-1A). Glyceraldehyde 3-phosphate

dehydrogenase (G3PDH) was amplified as a reference gene by using a sense primer

(5'-ACC ACA GTC CAT GCC ATC AC -3') and an antisense primer (5'-TCC ACC ACC

CTG TTG CTG TA-3') for normalization. Expression levels of luc2 or MOR-1A were

calculated as $2^{-\Delta\Delta C(t)}$ ($\Delta\Delta C(t) = \Delta C(t)_{luc2\ or\ MOR-1A} - \Delta C(t)_{G3PHD}$). For quantify miR-103

and miR-107, total RNAs extracted with miRNeasy Kit from cells or brain regions were

reverse-transcribed with Universal cDNA Synthesis Kit (Exiqon). The cDNA was then

used as template in SYBR green qPCR with SYBR green master mix and miR-103 or

miR-107 LNA primer set (Exiqon). U6 snRNA was amplified as a reference gene by

using U6 snRNA LNA primer set (Exiqon) for normalization. Expression level of miR-

13

103 and miR-107 was calculated as $2^{-\Delta\Delta C(t)}$ ($\Delta\Delta C(t) = \Delta C(t)_{\text{miR-107 or miR-103}} - \Delta C(t)_{\text{U6 snRNA}}$).

Receptor binding assay. Membrane isolation from transfected HEK293 cells and ^{125}I-Iodobenzoylnaltrexamide (IBNtxA) binding were performed as described previously(Majumdar et al., 2011a). Specific binding was defined as the difference between total binding and nonspecific binding, defined by levallorphan (1 µM). Protein concentration was determined by Lowry method using BSA as the standard. ^{125}I-IBNtxA had high affinity (K_D, 0.11 nM) toward mMOR-1 when expressed in CHO cells (Majumdar et al., 2011a).

Results

hMOR-1A and mMOR-1A contain a consensus poly(A) site in their 3'-UTR.

The initial hMOR-1A and mMOR-1A cDNA clones contained only partial 3'-UTR sequences with no information about their poly(A) and cleavage sites, the essential signals for terminating transcription and adding poly(A) tail in most eukaryotic genes. To identify the poly(A) site and complete 3'-UTR of hMOR-1A and mMOR-1A transcripts, we used a 3'RACE approach in which poly(A)-selected RNAs purified from Be(2)C cells and mouse brain were reverse-transcribed with a oligo(dT) primer flanking the unique sequences for anchoring two primers, AP1 and AP2, which allows unbiased amplification of the 3'-UTR containing poly(A) site by subsequent nested PCRs using the combination of AP1 and AP2 antisense primers with two specific sense primers (hA, hB, mA and mB) derived from exons 3a/3b (Fig. 2A). After two rounds of PCRs, we

14

obtained a ~ 500 bp PCR fragment in the human Be(2)C cells (Fig. 2B) and a ~ 850 bp

PCR fragment in the mouse brain (Fig. 2D). Sequence analysis of the PCR fragments

revealed a consensus poly(A) site, AAUAAA, located 15 bp and 5 bp upstream of a

common cleavage site, the CA dinucleotide, in hMOR-1A and mMOR-1A, respectively

(Figs. 2C, 2E & 2F). The total length of the 3'-UTR from the stop codon to the cleavage

site is 640 bases in hMOR-1A and 1,322 bases in mMRO-1A. The poly(A) and cleavage

sites were flanked by U-rich and/or G-rich sequences (Figs. 2C, 2E & 2F). All these cis-

elements including poly(A), cleavage site and U-rich/G-rich sequences are commonly

seen in a typical eukaryotic pre-mRNA 3' end, and provide the basis of the 3' end

processing including transcript cleavage and poly(A) addition for hMOR-1A and mMOR-

1A.

To verify the results from the 3' RACE, we analyzed the full-length hMOR-1A and

mMOR-1A transcripts using Northern blots with probes derived from regions upstream

or downstream of the poly(A) sites (Fig. 3A). Probe 2 derived from the 3'-UTR upstream

of the poly(A) region detected a major band of ~ 2 kb or ~ 3 kb in mRNAs from Be(2)C

cells or mouse brain, respectively (Figs. 3B & 3C) A probe from exon 3a (Probe 1) also

labeled bands with similar sizes. Thus, the lengths of hMOR-1A and mMOR-1A

transcripts revealed by Northern blots were consistent with those predicted from the 3'-

UTRs that were identified through the 3'RACE. Probe 1 also hybridized several

additional bands in both human and mouse associated with exon 3a, which present in a

number of additional variants. Of those, a major band of ~ 12 kb corresponds to the

original MOR-1 transcript identified using various probes since the human or mouse

exon 4 is ~ 10 – 11 kb. On the other hand, a probe derived from the region downstream

of the cleavage site failed to detect any specific bands, suggesting that this region is not

included in hMOR-1A and mMOR-1A transcripts and supporting the transcription

termination sites identified through the 3'RACE for hMOR-1A and mMOR-1A.

We then examined the role of the 3'-UTR in mRNA stability by using a reporter

assay in which the luciferase reporter activity was measured on a construct with or

without the 3'-UTR of hMOR-1A or mMOR-1A in HEK293 cells (Fig. 4A). We observed

that the luciferase activity of the construct without the 3'-UTRs or poly(A) signal

sequence (pNo-3'UTR) was ~ 4 – 6-fold lower than that of the construct with the 3'-UTR

(pH-3'UTR and pM-3'UTR, Fig. 4B). RT-PCR confirmed that the decreased luciferase

activity was mainly due to a marked decrease in luciferase mRNA (Fig. 4B), suggesting

that the 3'-UTR of both hMOR-1A and mMOR-1A play an important role in maintaining

mRNA stability, presumably through the consensus poly(A) site in their 3'-UTR .

miR-103/107 reduces expression of MOR-1A via its consensus binding site at

MOR-1A 3'-UTR

To identify potential miRNA targets in the hMOR-1A and mMOR-1A 3'-UTRs, we

scanned the sequences in several computer programs including RegRNA and

miRBase, and identified a conserved miR-103/107 targeting site in the 3'-UTR of both

hMOR-1A and mMOR-1A (Fig. 5A). The sequences of mature miR-103 and miR-107

differ by one nucleotide at position 21 (Fig. 5A). There was a perfect 7mer-seed match

of miR-103/107 with a 3'-UTR region of mMOR-1A, while a 6mer-seed match was found

with a 3'-UTR region of hMOR-1A. To examine whether these predicted miR-103/107

binding sites on the 3'-UTR's can be actually targeted by miR-103/107, we first

employed a mutagenesis approach to evaluate the role of the predicted miR-103/107

binding sites in a luciferase reporter assay in HEK293 cells that highly express miR-103

and miR-107 (Figs. 5B & 5C). The luciferase activities of the mutant constructs (Fig. 5C)

in which the predicted miR-103/107 binding site in the hMOR-1A or mMOR-1A 3'-UTR

was disrupted were significantly higher than those of the wild type (wt) constructs (Fig.

5D), suggesting that these predicted miR-103/107 sites function as a repressive

element, presumably mediated through the expressed miR-103 and miR-107 in

HEK293 cells.

We next used an antisense LNA oligo approach to downregulate miR-103 and

miR-107 and investigate the effect of the downregulation on luciferase activities with the

wt construct. To downregulate miR-103 and miR-107 in HEK293 cells, we initially

established transfection conditions, such as doses and duration, for an antisense LNA

oligo against both miR-103 and miR-107 (miR-107 inhibitor). The miR-107 inhibitor

efficiently downregulated expression of both miR-103 and miR-107 (Fig. 5E & F) at 48

hr after transfection, an optimal time based upon a time course study (data not shown).

The miR-107 inhibitor (7.5 nM) reduced miR-103 and miR-107 ~ 60% and ~ 57%,

respectively. Further increasing the dose (15 nM) did not significantly enhance the

effect. We therefore used the miR-107 inhibitor at 7.5 nM in co-transfection studies with

the human or mouse wt construct in HEK293 cells. Downregulating miR-103/107 with

the inhibitor significantly increased luciferase activity of both the human and mouse

constructs (Fig. 5G), suggesting that miR-103/107 functions as a repressor to regulate

luciferase activity through the predicted miR-103/107 binding sites in the hMOR-1A and

mMOR-1A 3'-UTRs. However, the increase in luc2 activity was modest, a ~ 22% (pM-

17

wt) and ~ 27% (pH-wt) of increase over the control oligo, and similar changes observed

with the mutant constructs (Fig. 5D). This probably indicated the actual effect of miR-

103/107 on luc2 activities in this particular context. We observed larger effects using

different constructs and assays (see below, Fig. 6).

miR-103/107 regulates MOR-1A expression at the post-transcriptional level

miRNAs regulate their target genes at translational level, but also at

transcriptional level. To assess the level miR-103/107 regulation of hMOR-1A and

mMOR-1A expression, we adopted an approach in which a polyribosome-associated

mRNA was quantified to determine its translation efficiency, while the steady-state total

mRNA level from the same cells was determined in parallel. We first made a construct

containing the entire coding region and complete 3'-UTR of hMOR-1A (ph1A/wt) or

mMOR-1A (pm1A/wt) whose expression is under the control of a cytomegalovirus

(CMV) promoter and a mutant construct that was identical to ph1A/wt or m1A/wt, except

that the miR-103/107 binding site in the 3'-UTR was disrupted in the same way as in the

luciferase constructs (Fig. 5C), as ph1A/mut or m1A/mut (Fig. 6A). When transfected

into HEK293 cells, the mutant construct (ph1A/mut) increased opioid binding over 54%

compared to the wt construct (ph1A/wt) (Fig. 6B), indicating that the miR-103/107

binding site functioned as a repressive element, in a similar manner as with the

luciferase constructs (Fig. 5D).

We then determined the mMOR-1A mRNA levels in both total RNA and

polyribosomal fractions in HEK293 cells transfected with the wt or mutant constructs by

RT-qPCR. We observed no significant changes of the mMOR-1A mRNA in the steady-

state total mRNAs between the wt and mutant constructs (Figs. 6C), suggesting that the miR-103/107 binding site did not influence the expression of mMOR-1A at the transcription and/or degradation level. However, the mMOR-1A mRNAs were increased in the polyribosomal fractions of the mutant constructs by ~190% as compared to the wt constructs (Figs. 6C), suggesting the post-transcriptional or translational repressive effects of the miR-103/107 binding sites on mMOR-1A expression in the luciferase assays and opioid binding assays. The downregulation of miR-103/107 by the miR-107 inhibitor increased the polyribosome-associated mMOR-1A by ~125% over the control LNA oligo, and did not affect on the steady-state total mMOR-1A mRNA (Fig. 6D).

Chronic morphine treatment upregulates miR-103 and miR-107 expression in Be(2)C cells and the mouse striatum.

Morphine regulates the expression of a number of miRNAs, such as miR-23b, miR-133b and let-7, in cell lines and in animals. To investigate whether morphine can regulate miR-103 and miR-107 expression, we examined miR-103 and miR-107 expression in morphine-treated Be(2)C cells. In Be(2)C cells, morphine increased miR-107 expression in a time- and dose-dependent manner (Figs 7A & 7B). Similarly, morphine significantly upregulated miR-103 expression (Fig. 7C).

We then examined expression of miR-103 and miR-107 in a morphine tolerant mouse model. Subcutaneous implantation of morphine pellet (75 mg free base) significantly enhanced expression levels of miR-103 and miR-107 in the striatum (Fig. 7D) in a manner similar to Be(2)C cells. This *in vivo* effect was region dependent, with

19

no significant change in miR-103 and miR-107 expression in the prefrontal cortex (PFC)

(Fig. 7D).

Chronic morphine treatment downregulates polyribosome-associated MOR-1A

via miR-103/107 in Be(2)C cells and the mouse striatum.

We next examined the effect of morphine on expression of endogenous hMOR-

1A in Be(2)C cells. Morphine treatment significantly decreased the polyribosome-

associated hMOR-1A mRNA in Be(2)C cells, (Lanes 5 & 6, Fig. 8A), suggesting that

morphine inhibits the hMOR-1A expression at translational or post-transcriptional level,

leading to translating less hMOR-1A protein. The decreased polyribosome-associated

hMOR-1A by morphine was clearly not contributed by the change of the steady-state

total hMOR-1A mRNA level. On the contrary the steady-state total hMOR-1A mRNA

level was actually increased by morphine (Lanes 1 & 2, Fig. 8A), suggesting that

morphine differentially regulates hMOR-1A expression at transcription and/or

degradation levels.

To examine whether the effect of morphine on the polyribosome-associated

hMOR-1A mRNA was mediated through miR-103/107 in Be(2)C cells, we used the miR-

107 inhibitor to downregulate miR-103 and miR-107 in morphine-treated Be(2)C cells.

The miR-107 inhibitor effectively reduced both miR-103 and miR-107 by ~75% and

~85%, respectively, in Be(2)C cells when compared to the control LNA oligo (Fig. 8B).

The miR-107 inhibitor did not affect the levels of steady-state total hMOR-1A mRNA

(Lanes 3 & 4, Fig. 8A). However, the miR-107 inhibitor significantly increased the

polyribosome-associated hMOR-1A mRNA in morphine-treated Be(2)C cells almost

50% higher than the control LNA oligo (Lanes 7 & 8, Fig. 8A), suggesting that the decrease in polyribosome-associated hMOR-1A mRNA by morphine was at least partly due to morphine's action on upregulating miR-103/107 (Figs. 7A & 7B). The miR-107 inhibitor did not completely reverse morphine's actions on the polyribosome-associated hMOR-1A mRNA (Lanes 5, 6 & 8, Fig. 8A). This may be due to other morphine actions, possibly involving additional miRNAs.

We also examined the effect of morphine on expression of endogenous exons 3 & 4 (hE3-4) mRNA that predominantly corresponds to hMOR-1 expression in Be(2)C cells. Unlike hMOR-1A, morphine treatment did not affect hE3-4 mRNA expression in the total RNA fraction, and showed a trend toward decreasing by ~10% polyribosome-associated hE3-4 mRNA, although it was not statistically significant (Fig. S1). On the other hand, the miR-107 inhibitor treatment increased the polyribosome-associated hE3-4 mRNA by over 50% as compared to the control LNA oligo treatment, and had no effect on hE3-4 mRNA level in the total RNA fraction (Fig. S1), suggesting that hMOR-1 is also regulated by miR-103/107 at the post-transcriptional level. Interestingly, computer modeling suggested several miR-103/107 binding sites in 3'-UTR of exon 4.

We further investigated the effect of morphine on the expression of mMOR-1A in the PFC and striatum of morphine tolerance mice. There were no significant change in mMOR-1A mRNA in both total RNA and polyribosome fractions in the PFC (Fig. 8C), consistent with no changes of miR-103/107 expression in the PFC in the same mouse model (Fig. 7D). However, chronic morphine treatment significantly decreased the polyribosome-associated mMOR-1A mRNA in the striatum without affecting the steady-state total mMOR-1A mRNA (Fig. 8C). Since morphine upregulated miR-103/107 in the

striatum (Fig. 7D), these data suggested that the *in vivo* effect of morphine on modulating the polyribosome-associated mMOR-1A mRNA in the striatum is most likely acted through miR-103/107 as it did in Be(2)C cells.

Discussion

The 3'-UTR plays crucial roles in many processes of gene regulation such as transcription, splicing, transport, translation and mRNA stability (Mandel et al., 2008;Elkon et al., 2013;Tian and Manley, 2013). To better understand gene regulation of the *OPRM1* splice variants, we isolated the complete 3'-UTR for one of dominant C-terminal splice variants in both human (hMOR-1A) and mouse (mMOR-1A) by 3' RACE, enabling us to explore the functions of the 3'-UTR. The 3'RACE and Northern blots indicated that a conserved major poly(A) signal and its associated cleavage site were used to terminate transcription of both hMOR-1A and mMOR-1A mRNA, although the lengths of the 3'-UTRs differed between hMOR-1A (~0.6 kb) and mMOR-1A (~1.3 kb). These cis-elements, together with the flanking U-rich and/or G-rich regions, are major components in pre-mRNA 3' end processing of most eukaryotic genes, and play important roles in regulating expressions of hMOR-1A and mMOR-1A mRNAs.

One major function of polyadenylation is to protect mRNA from degradation. Like the 3'-UTRs of other genes and the original mMOR-1 from the same gene, the 3'-UTRs of hMOR-1A and mMOR-1A greatly enhanced the stability of the luciferase mRNA in HEK293 cells using the luciferase reporter assay in which the expression of the constructs was under the control of an exogenous PGK promoter, through the conserved poly(A) signal and cleavage sites. Pre-mRNA 3' end processing is influenced

by promoter activity. When we replaced the PGK promoter with a ~ 2 kb endogenous

exon 1 promoter in the same reporter constructs, however, we observed much lower

luciferase activity in HEK293 cells compared to the PGK promoter (data not shown),

presumably due to limitation of the non-neuronal cell type we used and/or the

exogenous luciferase coding sequences. It will be interesting to further explore the

functional relationships between the endogenous promoter and 3' end processing in

expression of hMOR-1A and mMOR-1A mRNAs in neuronal cells.

The poly(A) sites of hMOR-1A and mMOR-1A can be considered as an intronic

polyadenylation site since they are located within the intron of other splice variants.

These variants have alternative downstream exons that presumably contain their own

poly(A) sites. A major poly(A) site was already identified in exon 4 mainly for terminating

the transcription of the original mMOR-1 and hMOR-1. In addition to the poly(A) sites of

hMOR-1A and mMOR-1A reported in the present study, we also identified a poly(A) site

in the 3'-UTR of the mMOR-1Bs (unpublished observation). We believe that the other

splice variants such as mMOR-1C, mMOR-1D, mMOR-1E, hMOR-1Bs, hMOR-1X,

hMOR-1Y and hMOR-1O have their own poly(A) sites. This raises intriguing questions

how these poly(A) sites spanning over 100 kb from exon 3 to exon 7 (mouse) or exon

O (human) or exon 8 (Fig. 1) are used in the context of transcription and splicing.

Growing evidence indicates that poly(A) sites play an important role in alternative

splicing(Tian et al., 2007;Vorlova et al., 2011;Licatalosi and Darnell, 2010). Particularly,

interconnection between polyadenylation and U1 small nuclear ribonucleoprotein

(snRNP) is one of the key mechanisms to determine the usage of 5' splice sites(Fortes

et al., 2003;Goraczniak et al., 2009;Gunderson et al., 1998;Kaida et al., 2010). In the

future, we hope to investigate the interaction between the poly(A) sites of hMOR-1A and

mMOR-1A and U1 snRNP and how these interactions influence the expression of

hMOR-1A and mMOR-1A mRNAs. This interaction may contribute, at least partly, to the

differential expression of mMOR-1A mRNA seen in various brain regions(Xu et al.,

2013).

miRNAs primarily target the 3'-UTR to regulate gene expression at both

translation and/or transcription levels, although 5'-UTR, coding and intronic regions also

can be involved. Our studies reveal that miR-103/107 targets a conserved miR-103/107

binding site in the 3'-UTR of hMOR-1A and mMOR-1A that was initially predicted from

the computer models. This conclusion is based upon the observations that disrupting

the miR-103/107 binding sequences in the 3'-UTRs by mutagenesis significantly

increases the exogenous luciferase activity in the luciferase assay and hMOR-1A

receptor expression in opioid binding assay in HEK293 cells and that downregulating

miR-103/107 in HEK293 cells with a miR-107 inhibitor enhances the luciferase activity

of the 3'-UTR constructs containing the miR-103/107 binding sites. We further illustrated

that miR-103/107 mainly functions at the post-transcriptional or translational level to

regulate MOR-1A expression, as shown by the increase in polyribosome-associated

MOR-1A mRNA when the mutant construct and miR-107 inhibitor were used, without

affecting steady-state mRNA levels. Previous studies indicated that several miRNAs

such as miR-23b and let-7 inhibit the expression of the original mMOR-1 at the post-

transcriptional level through their binding sites located at the 3'-UTR(Wu et al., 2009;Wu

et al., 2008;He et al., 2010). Our study shows for the first time that a pair of paralogous

miRNAs, miR-103 and miR-107, can regulate the expression of a C-terminal splice

variant at the post-transcriptional level through its 3'-UTR, as determined by measurement of polyribosome-associated mRNA. Different *OPRM1* splice variants presumably have diverse 3'-UTRs, leading to the question of the role of miRNAs on their expression. Extending the current studies to other variants may prove revealing.

Mature miR-103 and miR-107 have identical sequences except for one nucleotide at the 3'-end, and regulate overlapping targets(Trajkovski et al., 2011;Chen et al., 2012;Zhang et al., 2012). They are widely expressed in different tissues such as brain, liver, lung and heart(Baskerville and Bartel, 2005;Wang and Wang, 2006;Miska et al., 2004). Both miRNAs are transcribed from the introns of the pantothenate kinase family (PANK) genes that encode key regulatory enzymes in the biosynthesis of coenzyme A(Wilfred et al., 2007). Dysregulation of miR-103 and miR-107 occurs in a number of diseases including metabolic disorders(Trajkovski et al., 2011), cancer(Rottiers and Naar, 2012;Chen et al., 2012;Chen et al., 2013) and neuropathic pain(Favereaux et al., 2011).

Increasing evidence indicates that mu opioids such as morphine can regulate expression of a number of miRNAs. For example, chronic morphine treatment upregulates miR-23b in mouse neuronal N2A cells(Wu et al., 2009), and increases let-7 in SH-SY5Y cells and in morphine tolerant mouse brain (He et al., 2010). Our study provides another example where morphine increases miR-103/107 expression in both Be(2)C cells and the striatum of the morphine tolerant mouse. Since genomic locations of both miRNAs are located in PANK genes, it is speculated that the morphine-induced miR-103 and miR-107 increase may be contributed by morphine actions on transcription of PANK genes. The increased miR-103/107 induced by morphine was at least partially

responsible for morphine action on reducing polyribosome-associated hMOR-1A mRNA in Be(2)C cells. Similar effects of morphine on the expression of miR-103/107 and mMOR-1A were observed in the morphine tolerant mouse model in which morphine increased miR-103/107 and decreased the polyribosome-associated mMOR-1A mRNA in the striatum with no changes in the PFC. Several miRNAs have been shown to play an important role in developing morphine tolerance in mice. For example, downregulating let-7 by a LNA antisense oligo leads to increase of mMOR-1 protein and reduction of morphine tolerance(He et al., 2010). Our finding raises another possibility that the interplay between miR-103/107 and mMOR-1A may contribute to the development of morphine tolerance in mice.

Authorship Contributions:

Participated in research design: Lu, Pasternak and Pan.

Conducted experiments: Lu, Xu (J), Xu (M), and Pan.

Contributed new reagents or analytic tools: Lu, and Xu(J).

Performed data analysis: Lu, and Pan.

Wrote or contributed to the writing of the manuscript: Lu, Pasternak and Pan.

References

Abbadie C, Pan Y X, Drake C T and Pasternak G W (2000a) Comparative Immunohistochemical Distributions of Carboxy Terminus Epitopes From the Mu-Opioid Receptor Splice Variants MOR-1D, MOR-1 and MOR-1C in the Mouse and Rat CNS. *Neuroscience* 100:141-153.

Abbadie C, Pan Y X and Pasternak G W (2000b) Differential Distribution in Rat Brain of Mu Opioid Receptor Carboxy Terminal Splice Variants MOR-1C-Like and MOR-1-Like Immunoreactivity: Evidence for Region-Specific Processing. *J Comp Neurol* 419:244-256.

Abbadie C, Pasternak G W and Aicher S A (2001) Presynaptic Localization of the Carboxy-Terminus Epitopes of the Mu Opioid Receptor Splice Variants MOR-1C and MOR-1D in the Superficial Laminae of the Rat Spinal Cord. *Neuroscience* 106:833-842.

Bare LA, Mansson E and Yang D (1994) Expression of Two Variants of the Human m Opioid Receptor MRNA in SK-N-SH Cells and Human Brain. *FEBS Lett* 354:213-216.

Baskerville S and Bartel D P (2005) Microarray Profiling of MicroRNAs Reveals Frequent Coexpression With Neighboring MiRNAs and Host Genes. *RNA* 11:241-247.

Bolan EA, Pan Y X and Pasternak G W (2004) Functional Analysis of MOR-1 Splice Variants of the Mouse Mu Opioid Receptor Gene Oprm. *Synapse* 51:11-18.

Chen HY, Lin Y M, Chung H C, Lang Y D, Lin C J, Huang J, Wang W C, Lin F M, Chen Z, Huang H D, Shyy J Y, Liang J T and Chen R H (2012) MiR-103/107 Promote Metastasis of Colorectal Cancer by Targeting the Metastasis Suppressors DAPK and KLF4. *Cancer Res* 72:3631-3641.

Chen L, Chen X R, Chen F F, Liu Y, Li P, Zhang R, Yan K, Yi Y J, Xu Z M and Jiang X D (2013) MicroRNA-107 Inhibits U87 Glioma Stem Cells Growth and Invasion. *Cell Mol Neurobiol* 33:651-657.

Dave RS and Khalili K (2010) Morphine Treatment of Human Monocyte-Derived Macrophages Induces Differential MiRNA and Protein Expression: Impact on Inflammation and Oxidative Stress in the Central Nervous System. *J Cell Biochem* 110:834-845.

Dreyer JL (2010) New Insights into the Roles of MicroRNAs in Drug Addiction and Neuroplasticity. *Genome Med* 2:92.

Elkon R, Ugalde A P and Agami R (2013) Alternative Cleavage and Polyadenylation: Extent, Regulation and Function. *Nat Rev Genet* 14:496-506.

Favereaux A, Thoumine O, Bouali-Benazzouz R, Roques V, Papon M A, Salam S A, Drutel G, Leger C, Calas A, Nagy F and Landry M (2011) Bidirectional Integrative

Regulation of Cav1.2 Calcium Channel by MicroRNA MiR-103: Role in Pain. *EMBO J* 30:3830-3841.

Fortes P, Cuevas Y, Guan F, Liu P, Pentlicky S, Jung S P, Martinez-Chantar M L, Prieto J, Rowe D and Gunderson S I (2003) Inhibiting Expression of Specific Genes in Mammalian Cells With 5' End-Mutated U1 Small Nuclear RNAs Targeted to Terminal Exons of Pre-MRNA. *Proc Natl Acad Sci U S A* 100:8264-8269.

Giros B, Pohl M, Rochelle J M and Seldin M F (1995) Chromosomal Localization of Opioid Peptide and Receptor Genes in the Mouse. *Life Sci* 56:PL369-PL375.

Goraczniak R, Behlke M A and Gunderson S I (2009) Gene Silencing by Synthetic U1 Adaptors. *Nat Biotechnol* 27:257-263.

Gunderson SI, Polycarpou-Schwarz M and Mattaj I W (1998) U1 SnRNP Inhibits Pre-MRNA Polyadenylation Through a Direct Interaction Between U1 70K and Poly(A) Polymerase. *Mol Cell* 1:255-264.

He Y, Yang C, Kirkmire C M and Wang Z J (2010) Regulation of Opioid Tolerance by Let-7 Family MicroRNA Targeting the Mu Opioid Receptor. *J Neurosci* 30:10251-10258.

Hwang CK, Wagley Y, Law P Y, Wei L N and Loh H H (2012) MicroRNAs in Opioid Pharmacology. *J Neuroimmune Pharmacol* 7:808-819.

Ide S, Han W, Kasai S, Hata H, Sora I and Ikeda K (2005) Characterization of the 3' Untranslated Region of the Human Mu-Opioid Receptor (MOR-1) MRNA. *Gene* 364:139-145.

Kaida D, Berg M G, Younis I, Kasim M, Singh L N, Wan L and Dreyfuss G (2010) U1 SnRNP Protects Pre-MRNAs From Premature Cleavage and Polyadenylation. *Nature* 468:664-668.

Koch T, Schulz S, Pfeiffer M, Klutzny M, Schroder H, Kahl E and Hollt V (2001) C-Terminal Splice Variants of the Mouse Mu-Opioid Receptor Differ in Morphine-Induced Internalization and Receptor Resensitization. *J Biol Chem* 276:31408-31414.

Koch T, Schulz S, Schroder H, Wolf R, Raulf E and Hollt V (1998) Carboxyl-Terminal Splicing of the Rat Mu Opioid Receptor Modulates Agonist-Mediated Internalization and Receptor Resensitization. *J Biol Chem* 273:13652-13657.

Kolesnikov YA, Pick C G, Ciszewska G and Pasternak G W (1993) Blockade of Tolerance to Morphine but Not to Kappa Opioids by a Nitric Oxide Synthase Inhibitor. *Proc Natl Acad Sci USA* 90:5162-5166.

Liang Y, Mestek A, Yu L and Carr L G (1995) Cloning and Characterization of the Promoter Region of the Mouse m Opioid Receptor Gene. *Brain Res* 679:82-88.

Licatalosi DD and Darnell R B (2010) RNA Processing and Its Regulation: Global Insights into Biological Networks. *Nat Rev Genet* 11:75-87.

Liu XY, Liu Z C, Sun Y G, Ross M, Kim S, Tsai F F, Li Q F, Jeffry J, Kim J Y, Loh H H and Chen Z F (2011) Unidirectional Cross-Activation of GRPR by MOR1D Uncouples Itch and Analgesia Induced by Opioids. *Cell* 147:447-458.

Majumdar S, Burgman M, Haselton N, Grinnell S, Ocampo J, Pasternak A R and Pasternak G W (2011a) Generation of Novel Radiolabeled Opiates Through Site-Selective Iodination. *Bioorg Med Chem Lett* 21:4001-4004.

Majumdar S, Grinnell S, Le R, V, Burgman M, Polikar L, Ansonoff M, Pintar J, Pan Y X and Pasternak G W (2011b) Truncated G Protein-Coupled Mu Opioid Receptor MOR-1 Splice Variants Are Targets for Highly Potent Opioid Analgesics Lacking Side Effects. *Proc Natl Acad Sci U S A* 108:19778-19783.

Mandel CR, Bai Y and Tong L (2008) Protein Factors in Pre-MRNA 3'-End Processing. *Cell Mol Life Sci* 65:1099-1122.

Min BH, Augustin L B, Felsheim R F, Fuchs J A and Loh H H (1994) Genomic Structure and Analysis of Promoter Sequence of a Mouse m Opioid Receptor Gene. *Proc Natl Acad Sci USA* 91:9081-9085.

Miska EA, Alvarez-Saavedra E, Townsend M, Yoshii A, Sestan N, Rakic P, Constantine-Paton M and Horvitz H R (2004) Microarray Analysis of MicroRNA Expression in the Developing Mammalian Brain. *Genome Biol* 5:R68.

Pan L, Xu J, Yu R, Xu M M, Pan Y X and Pasternak G W (2005a) Identification and Characterization of Six New Alternatively Spliced Variants of the Human Mu Opioid Receptor Gene, Oprm. *Neuroscience* 133:209-220.

Pan YX (2005) Diversity and Complexity of the Mu Opioid Receptor Gene: Alternative Pre-MRNA Splicing and Promoters. *DNA Cell Biol* 24:736-750.

Pan YX, Xu A, Mahurter L, Bolan E, Xu M M and Pasternak G W (2001) Generation of the Mu Opioid Receptor (MOR-1) Protein by Three New Splice Variants of the Oprm Gene. *Proc Natl Acad Sci USA* 98:14084-14089.

Pan YX, Xu J, Bolan E, Abbadie C, Chang A, Zuckerman A, Rossi G and Pasternak G W (1999) Identification and Characterization of Three New Alternatively Spliced Mu-Opioid Receptor Isoforms. *Mol Pharmacol* 56:396-403.

Pan YX, Xu J, Bolan E, Moskowitz H S, Xu M and Pasternak G W (2005b) Identification of Four Novel Exon 5 Splice Variants of the Mouse Mu-Opioid Receptor Gene: Functional Consequences of C-Terminal Splicing. *Mol Pharmacol* 68:866-875.

Pan YX, Xu J, Xu M, Rossi G C, Matulonis J E and Pasternak G W (2009) Involvement of Exon 11-Associated Variants of the Mu Opioid Receptor MOR-1 in Heroin, but Not Morphine, Actions. *Proc Natl Acad Sci U S A* 106:4917-4922.

Pasternak DA, Pan L, Xu J, Yu R, Xu M M, Pasternak G W and Pan Y X (2004) Identification of Three New Alternatively Spliced Variants of the Rat Mu Opioid Receptor Gene: Dissociation of Affinity and Efficacy. *J Neurochem* 91:881-890.

Pasternak GW (1993) Pharmacological Mechanisms of Opioid Analgesics. *Clin Neuropharmacol* 16:1-18.

Pasternak GW and Pan Y-X. (2013) Mu Opioids and Their Receptors: Evolution of a Concept. *Pharmacol Rev* 65:1-61.

Reisine T and Pasternak G W (1996) Opioid analgesics and antagonists, in *Goodman & Gilman's: The Pharmacological Basis of Therapeutics* (Hardman JG and Limbird LE eds) pp 521-556, McGraw-Hill.

Rossi GC, Brown G P, Leventhal L, Yang K and Pasternak G W (1996) Novel Receptor Mechanisms for Heroin and Morphine-6b -Glucuronide Analgesia. *Neurosci Lett* 216:1-4.

Rossi GC, Leventhal L, Pan Y X, Cole J, Su W, Bodnar R J and Pasternak G W (1997) Antisense Mapping of MOR-1 in the Rat: Distinguishing Between Morphine and Morphine-6b-Glucuronide Antinociception. *J Pharmacol Exp Ther* 281:109-114.

Rossi GC, Pan Y-X, Brown G P and Pasternak G W (1995) Antisense Mapping the MOR-1 Opioid Receptor: Evidence for Alternative Splicing and a Novel Morphine-6b-Glucuronide Receptor. *FEBS Lett* 369:192-196.

Rottiers V and Naar A M (2012) MicroRNAs in Metabolism and Metabolic Disorders. *Nat Rev Mol Cell Biol* 13:239-250.

Sanchez-Simon FM, Zhang X X, Loh H H, Law P Y and Rodriguez R E (2010) Morphine Regulates Dopaminergic Neuron Differentiation Via MiR-133b. *Mol Pharmacol* 78:935-942.

Schuller AGP, King M A, Zhang J W, Bolan E, Pan Y X, Morgan D J, Chang A, Czick M E, Unterwald E M, Pasternak G W and Pintar J E (1999) Retention of Heroin and Morphine-6 Beta-Glucuronide Analgesia in a New Line of Mice Lacking Exon 1 of MOR-1. *Nat Neurosci* 2:151-156.

Tanowitz M, Hislop J N and von Z M (2008) Alternative Splicing Determines the Post-Endocytic Sorting Fate of G-Protein-Coupled Receptors. *J Biol Chem* 283:35614-35621.

Tapocik JD, Luu T V, Mayo C L, Wang B D, Doyle E, Lee A D, Lee N H and Elmer G I (2012) Neuroplasticity, Axonal Guidance and Micro-RNA Genes Are Associated With Morphine Self-Administration Behavior. *Addict Biol* 18:480-495

Thoreen CC, Chantranupong L, Keys H R, Wang T, Gray N S and Sabatini D M (2012) A Unifying Model for MTORC1-Mediated Regulation of MRNA Translation. *Nature* 485:109-113.

Tian B and Manley J L (2013) Alternative Cleavage and Polyadenylation: the Long and Short of It. *Trends Biochem Sci* 38:312-320.

Tian B, Pan Z and Lee J Y (2007) Widespread MRNA Polyadenylation Events in Introns Indicate Dynamic Interplay Between Polyadenylation and Splicing. *Genome Res* 17:156-165.

Trajkovski M, Hausser J, Soutschek J, Bhat B, Akin A, Zavolan M, Heim M H and Stoffel M (2011) MicroRNAs 103 and 107 Regulate Insulin Sensitivity. *Nature* 474:649-653.

Vorlova S, Rocco G, Lefave C V, Jodelka F M, Hess K, Hastings M L, Henke E and Cartegni L (2011) Induction of Antagonistic Soluble Decoy Receptor Tyrosine Kinases by Intronic PolyA Activation. *Mol Cell* 43:927-939.

Wang X and Wang X (2006) Systematic Identification of MicroRNA Functions by Combining Target Prediction and Expression Profiling. *Nucleic Acids Res* 34:1646-1652.

Wang X, Ye L, Zhou Y, Liu M Q, Zhou D J and Ho W Z (2011) Inhibition of Anti-HIV MicroRNA Expression: a Mechanism for Opioid-Mediated Enhancement of HIV Infection of Monocytes. *Am J Pathol* 178:41-47.

Wilfred BR, Wang W X and Nelson P T (2007) Energizing MiRNA Research: a Review of the Role of MiRNAs in Lipid Metabolism, With a Prediction That MiR-103/107 Regulates Human Metabolic Pathways. *Mol Genet Metab* 91:209-217.

Wolozin BL and Pasternak G W (1981) Classification of Multiple Morphine and Enkephalin Binding Sites in the Central Nervous System. *Proc Natl Acad Sci U S A* 78:6181-6185.

Wu J and Bag J (1998) Negative Control of the Poly(A)-Binding Protein MRNA Translation Is Mediated by the Adenine-Rich Region of Its 5'-Untranslated Region. *J Biol Chem* 273:34535-34542.

Wu Q, Hwang C K, Yao S, Law P Y, Loh H H and Wei L N (2005) A Major Species of Mouse Mu-Opioid Receptor MRNA and Its Promoter-Dependent Functional Polyadenylation Signal. *Mol Pharmacol* 68:279-285.

Wu Q, Hwang C K, Zheng H, Wagley Y, Lin H Y, Kim D K, Law P Y, Loh H H and Wei L N (2013) MicroRNA 339 Down-Regulates Mu-Opioid Receptor at the Post-Transcriptional Level in Response to Opioid Treatment. *FASEB J* 27:522-535

Wu Q, Law P Y, Wei L N and Loh H H (2008) Post-Transcriptional Regulation of Mouse Mu Opioid Receptor (MOR1) Via Its 3' Untranslated Region: a Role for MicroRNA23b. *FASEB J* 22:4085-4095.

Wu Q, Zhang L, Law P Y, Wei L N and Loh H H (2009) Long-Term Morphine Treatment Decreases the Association of Mu-Opioid Receptor (MOR1) MRNA With Polysomes Through MiRNA23b. *Mol Pharmacol* 75:744-750.

Xu, J, Xu, M, Bolan, E, Gilbert, A. K, Pasternak, G. W., and Pan, Y-X (2013) Isolating and characterizing three alternatively spliced mu opioid receptor variants: mMOR-1A, mMOR-1O and mMOR-1P. Synapse In press.

Zhang SY, Surapureddi S, Coulter S, Ferguson S S and Goldstein J A (2012) Human CYP2C8 Is Post-Transcriptionally Regulated by MicroRNAs 103 and 107 in Human Liver. *Mol Pharmacol* 82:529-540.

Zheng H, Chu J, Zeng Y, Loh H H and Law P Y (2010) Yin Yang 1 Phosphorylation Contributes to the Differential Effects of Mu-Opioid Receptor Agonists on MicroRNA-190 Expression. *J Biol Chem* 285:21994-22002.

Figure Legends:

Fig. 1. Schematic of *OPRM1* gene structure and MOR-1A splice variants. MOR-1A variants from the human (A), mouse (B) and rat (C) *OPRM1* genes. Exons and introns are shown by colored boxes and black horizontal lines, respectively. Promoters are indicated by arrows. Exons are numbered in the order in which they were identified. Translation start and stop points are shown by bars below and above exon boxes, respectively. The complete list of the mouse *OPRM1* alternative splicing was described in the reviews (Pan, 2005;Pasternak and Pan Y-X., 2013).

Fig. 2. Cloning 3'-UTRs of hMOR-1A and mMOR-1A by 3' RACE. A. Schematic of the 3' RACE strategy. The 3'RACE was performed as described in Materials and Methods. Primers were shown by arrows. B & D. Analysis of PCR products on agarose gel. The 1st – and 2nd–round PCR products of hMOR-1A (B) and mMOR-1A (D) were separated on 1.5% agarose gel and stained with ethidium bromide. The gel was imaged with ChemiDoc MP System. Lanes 1 & 3: the 1st –round PCR products; Lanes 2 & 4: the 2nd –round PCR products. C & E. Partial cDNA sequences of the PCR fragments for hMOR-1A (C) and mMOR-1A (E). Poly(A) signal and cleavage sites are indicated by underlined red and bold letters. F. Alignment of the 3'-UTRs of hMOR-1A and mMOR-1A. poly(A) signal and cleavage sites are shown by red letters. U-rich or U/G-rich regions are indicated by black lines.

Fig. 3. Northern blot analysis. A. Schematic of the 3'-UTRs of hMOR-1A and mMOR-1A and relative positions of the probes. B & C. Northern blots. Northern blot analysis for

hMOR-1A (B) and mMOR-1A (C) was performed using poly(A) plus RNAs from Be(2)C

cells and mouse brain, as described in Materials and Methods. The full length

transcripts of hMOR-1A (~ 2 kb) and mMOR-1A (~ 3 kb) are shown by arrows.

Fig. 4. Role of the 3'-UTR of hMOR-1A and mMOR-1A in stabilizing luciferase mRNA.

A. Schematic of the plasmid constructs. The complete 3'-UTR of hMOR-1A and mMOR-

1A containing poly(A), cleavage site and U/G-rich region was subcloned into

downstream of the firefly luciferase (luc2) coding region, as pH-3'UTR and pM-3'UTR,

respectively, as described in Materials and Methods. Phosphoglycerate kinase (PGK)

promoter driving the transcription is shown by arrows. B. The Luc2 activity and mRNA

level of the transfected constructs. The lysates from transfected HEK293 cells with

indicated constructs were used for analyzing luc2 activity by using Dual-Glo Luciferase

Assay, as described in Materials and Methods. Total RNAs isolated from the transfected

cells were used in RT-PCR to determine expression of luc2 mRNA, as described in

Materials and Methods. Significant difference was calculated by one-way ANOVA with

Tukey's post hoc analysis. Compared with pNo-3'UTR, ***: $p < 0.001$; compared with

pM-3'UTR, ##: $p < 0.01$.

Fig. 5. Regulation of luciferase activity by miR-103/107 through a conserved miR-

103/107 binding site in MOR-1A 3'-UTRs. A. Alignment of miR-103 and miR-107

sequences with hMOR-1A and mMOR-1A 3'-UTRs. miR-103/107 seed and aligned 3'-

UTR sequences were shown by red letters. The positions of the 3'-UTRs relative to the

stop codons were indicated at the 3'-ends. B. Schematic of pmir constructs. The 3'-

UTRs of hMOR-1A and mMOR-1A containing wt or mutated miR-103/107 (miR-103/7) binding site were subcloned into pmir plasmid as pH-wt, pM-wt, pH-mut and pM-mut, respectively, as described in Materials and Methods. The wt and mutated miR-103/7 binding sites are indicated by red and green lines, respectively. C. Mutagenized sequences of the miR-103/7 binding sites in pmir constructs. Mutagenized sequences were indicacted by green letters. S represents G or C in miR-103/7 sequences. D. Effect of the mutation of the miR-103/7 binding site on the luciferase activity. Transfection of indicated constructs and measurement of luciferase activity were described in Materials and Methods. Fold change of luc2 activity was calculated by normalizing the values of the mutant constructs with those of the wt constructs. Compared with pH-wt, ***: $p < 0.001$; Compared with pM-wt, **: $p < 0.01$(Student t-test). E & F. Effect of miR-107 inhibitor on expression of miR-103 (E) and miR-107 (F) in HEK 293 cells. Transfection of miR-107 inhibitor into HEK293 cells using indicated concentrations and determination of miR-107 level by RT-qPCR were as described in Materials and Methods. Fold inhibition by miR-107 inhibitor was calculated by normalizing the levels with inhibitor with those with a control LNA oligo. Compared with Control LNA oligo, , *: $p < 0.05$; **: $p < 0.01$ and ***: $p < 0.001$ (Student t-test). G. Effect of miR-107 inhibitor on the luciferase activity in HEK293 cells. miR-107 inhibitor or Control LNA oligo was co-transfected with pH-wt or pM-wt construct into HEK293 cells as described in Materials and Methods. Fold change of luc2 activity was calculated by normalizing the values of the miR-107 inhibitor with those of the Control LNA oligo. Compared with Control LNA oligo, **: $p < 0.01$ and *: $p < 0.05$ (Student t-test).

Fig. 6. Inhibition of MOR-1A expression by miR-103/107 at post-transcriptional level.

A. Schematic of pcDNA3 constructs. The constructs containing the coding sequences

and 3'-UTRs of hMOR-1A and mMOR-1A with wt (red line) or mutated miR-103/7

binding site (green line) that were same as those in pmir constructs (Fig. 5C) were

made as described in Materials and Methods. B. Effect of the mutation on opioid

binding. Transfection of indicated constructs, membrane isolation and ^{125}I-IBNtxA

binding were described in Materials and Methods. Compared with ph1A/wt, *: p < 0.05.

C. Effect of miR-103/7 binding site on expression of mMOR-1A mRNA in HEK293 cells.

Isolation of total RNA and polyribosomal (polysomal) fraction, RNA extraction from

polysomal fraction and whole cells and RT-qPCR were described in Materials and

Methods. Expression of mMOR-1A mRNA was calculated by normalizing the level of

pm1A/mut with that of pm1A/wt. Compared with pm1A/wt, *: p < 0.05. D. Effect of miR-

107 inhibitor on expression of mMOR-1A mRNA in HEK293 cells. miR-107 inhibitor

(7.5nM) or Control LNA oligo (7.5nM) was co-transfected with pm1A/wt into HEK293

cells. Expression of mMOR-1A mRNA was calculated by normalizing the level of miR-

107 inhibitor with that of Control LNA oligo (Control). Compared with Control LNA oligo,

*: p < 0.05. Student t-test was used.

Fig. 7. Effect of chronic morphine on miR-107 expression in Be(2)C cells and morphine

tolerant mice. A. Effect of morphine on miR-107 expression at various times in Be(2)C

cells. Morphine treatment (3 µM) at indicated times and miR-107 expression determined

by RT-qPCR were described in Materials and Methods. Expression of miR-107 is

indicated by Fold changes calculated by normalizing with the level of 0 hour (hr). One-

way ANOVA was used for analyzing statistical significance. Compared with 0 hr, *: $p <$ 0.05; ***: $p < 0.001$; Compared with 12 hr, #: $p < 0.05$; ###: $p < 0.001$; Compared with 24 hr, $\Delta\Delta$: $p < 0.01$. B. Effect of morphine on miR-107 expression at various concentrations in Be(2)C cells. Expression of miR-107 was determined by RT-qPCR in Be(2)C cells treated with indicated concentrations of morphine for 48 hr. Fold changes were calculated by normalizing with the level of 0 µM. Compared with 0 µM, ***: $p <$ 0.001; Compared with 0.3 µM, ###: $p < 0.001$; Compared with 0.9 µM, Δ: $p < 0.05$. C. Effect of morphine on miR-103 expression in Be(2)C cells. Be(2)C cells were treated with 3 µM of morphine for 48 hr. miR-103 expression was determined by RT-qPCR as described in Materials and Methods. **: compared with no morphine treatment (Control), $p < 0.01$. D. Effect of morphine on miR-103 and miR-107 expression in the PFC and striatum of the morphine tolerant mouse model. Expression of miR-103 and miR-107 was determined by RT-qPCR in the PFC and striatum of a morphine tolerant mouse model implanted with s.c. morphine pellet (75 mg) (Morphine) or placebo pellet (Control), as described in Materials and Methods. Student t-test was used to analyze statistical difference. Compared with Control, *: $p < 0.05$.

Fig. 8. Effect of morphine on expression of MOR-1A via interaction between miR-103/107 and the MOR-1A 3'-UTRs. A. Effect of morphine on expression of hMOR-1A in Be(2)C cells. Expression of hMOR-1A was determined by RT-qPCR in total RNA and polyribosomal (polysomal) fraction of Be(2)C cells treated with or without 3 µM morphine and transfected with 5 nM miR-107 inhibitor or Control LNA oligo for 48 hr, as described in Materials and Methods. Expression level of hMOR-1A was calculated by

normalizing with the levels of the cells without any treatment (Lane 1 or 5). One-way

ANOVA was used to analyze statistical difference. Compared with Lane 1 or 5, ***: p <

0.001; **: p < 0.01. Compared with Lane 8, #: p < 0.05. B. Effect of miR-107 inhibitor on

miR-103 and miR-107 expression in Be(2)C cells. miR-103 and miR-107 expression

was determind by RT-qPCR in miR-107 inhibitor-treated Be(2)C cells (see A), as

described in Materials and Methods. Fold inhibition by the miR-107 inhibitor was

calculated by normalizing the levels with inhibitor with those with a control LNA oligo.

Compared with Control LNA oligo, **: p < 0.01; ***: p < 0.001. C. Effect of morphine on

expression of mMOR-1A in the PFC and striatum of the morphine tolerant mice.

Isolation of total RNA and polysomal mRNA and RT-qPCR for mMOR-1A was

described in Materials and Methods. Student t-test was used. Compared with Control

(placebo pellet), *: p < 0.05.
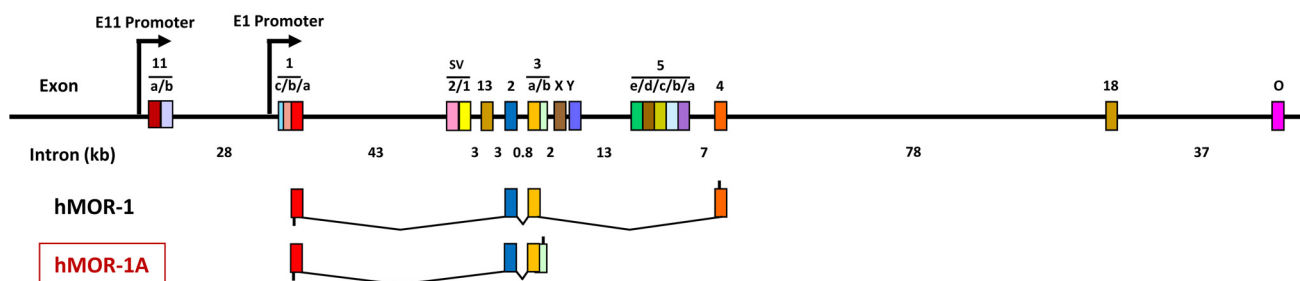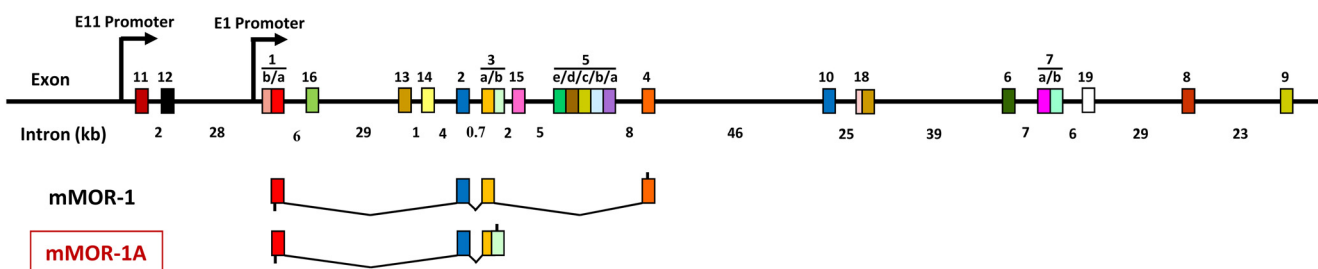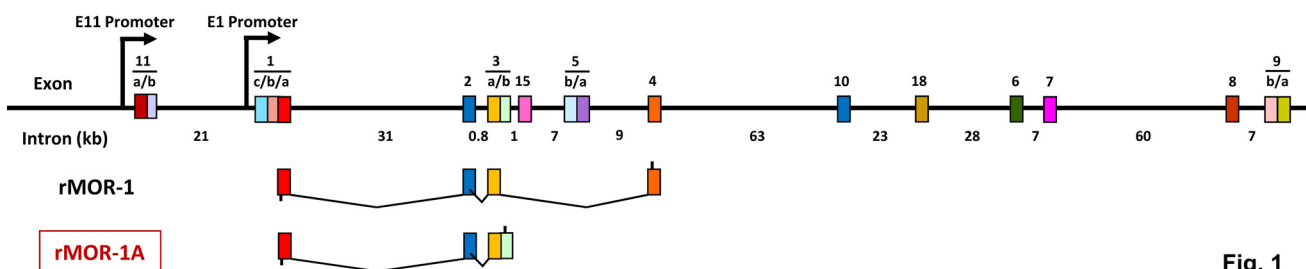
Fig. 1

A

3'RACE strategy for hMOR-1A
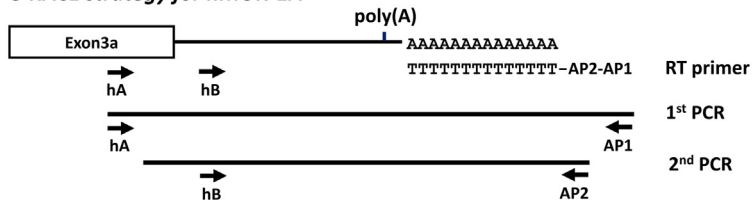
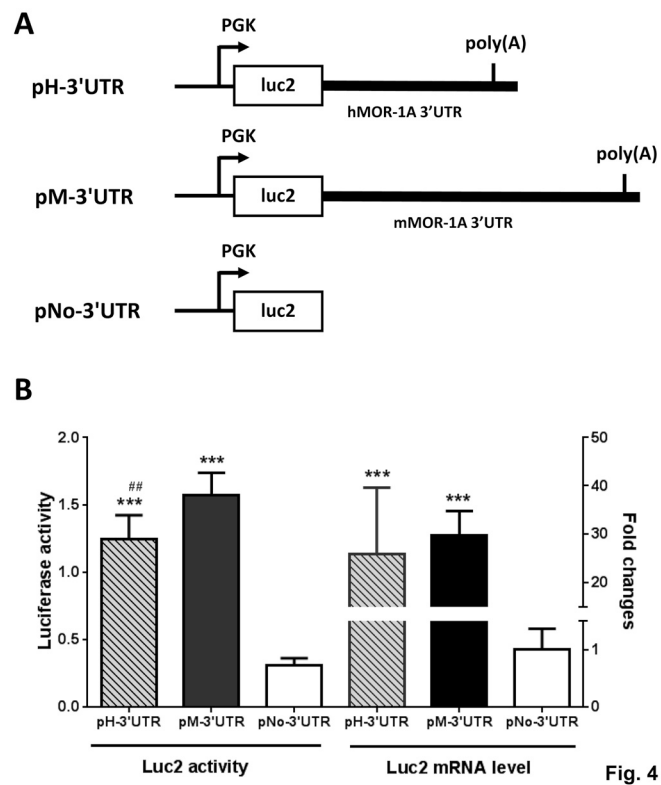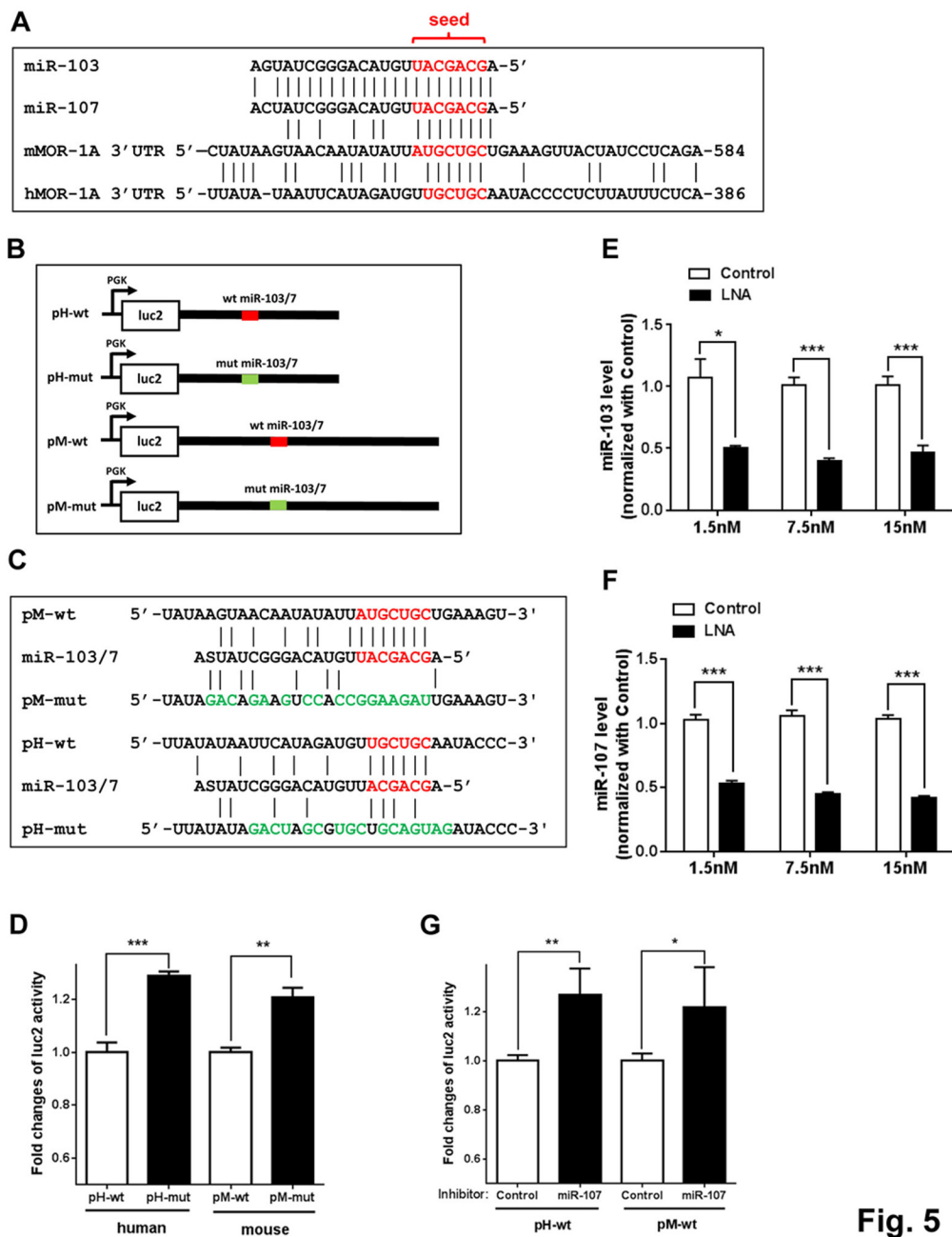*3'RACE strategy for mMOR-1A*

B

C

D

E

human MOR-1A

mouse MOR-1A

F

Fig. 2

Fig. 3

Fig. 4

Fig. 5

Fig. 6

Fig. 7

Fig. 8